

New Analysis Method for Adsorption in Gas (H₂, CO)–Solid (SnO₂) Systems Based on Gas Sensing

Xi-Tao Yin,* Ying Liu, Xiao-Ming Tan, Xiao-Chun Gao, Jing Li,* and Xiaoguang Ma*



Cite This: *ACS Omega* 2022, 7, 21262–21266



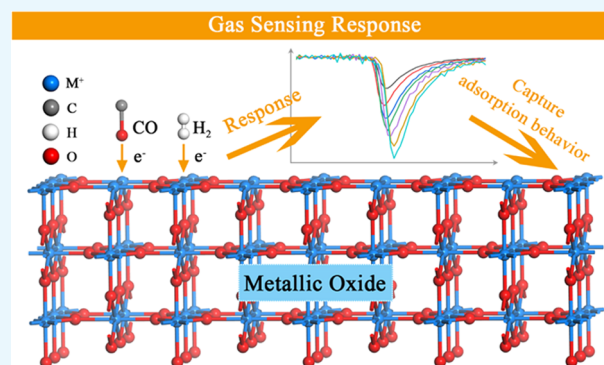
Read Online

ACCESS |

Metrics & More

Article Recommendations

ABSTRACT: The chemisorption phenomenon is widely used in the explanation of catalysis, gas–solid reactions, and gas sensing mechanisms. Generally, some properties of adsorbents, such as adsorption sites and dispersion, can be predicted by traditional methods through the variation of the chemisorption capacity with the temperature, pressure, and gas–solid interaction potential. However, these methods could not capture the information of the interaction between adsorbents, the adsorption rate, and the competitive adsorption relationship between adsorbents. In this paper, metal oxide semiconductors (MOSs) are employed to study the adsorption behavior. The gas sensing responses (GSRs) of MOSs caused by the gas adsorption process are measured as a new method to capture some adsorption behaviors, which are impossible for the traditional methods to obtain. The following adsorption behaviors characterized by this new method are presented for the first time: (1) distinguishing the adsorption type using an example of two reducing gases: the adsorption type of the two gases is single-molecular layer adsorption in this work; (2) detecting the interaction between different gases: this will be a promising method to provide original characterization data in the fields of gas–solid reaction mechanisms and heterogeneous catalysis; and (3) measuring the adsorption rate based on the GSR.



1. INTRODUCTION

MOS-based materials have been extensively used for gas sensor application.^{1–3} Their operating mechanism can be simply formulated as follows. Oxidizing gases such as O₂ adsorbed on the surface of SnO₂ can capture free electrons from its conductivity band, which increases the electrical conductivity. Oppositely, reducing gases such as H₂ and CO adsorbed on the surface of SnO₂ can produce free electrons, which increases the electrical conductivity so as to achieve the purpose of gas detection.^{4–10} It is commonly accepted that the essence of the sensing behavior is the process of adsorption.

Otherwise, polyphase (gas–solid) catalysis converts reactant molecules into reaction products through a cycle of elementary steps. The catalytic process includes at least five steps: diffusion, adsorption, surface reaction, desorption, and reverse diffusion. Among them, adsorption is the most important link in the process of polyphase catalysis.^{11,12} Furthermore, the adsorption of reactant molecules on the catalyst surface determines the extent to which the reactant molecules are activated and the properties of the catalytic process, such as activity and selectivity. Also, adsorption can also be important evidence to analyze the gas–solid reaction mechanism.¹³ Therefore, it is of great significance to study the adsorption using a new method.

Over the years, researchers have used a variety of modern spectroscopy technologies including various spectroscopic techniques and surface morphology detection techniques to obtain the adsorption behavior.^{14–16} Among them, the in situ experimental method mainly adopts the programmed temperature analysis technique (TPAT) to study the chemical adsorption behavior. Programmed temperature-rise technology mainly includes programmed temperature-rise desorption (TPD), reduction (TPR), oxidation (TPO), and surface reaction (TPSR). This technique characterizes the adsorption behavior by the change of the gas adsorption quantity during the adsorption or desorption process. However, there is another important characteristic in the process of adsorption: the exchange or coexistence of electrons between the gas adsorbent and solid surface; due to the existence of an uneven field on the solid surface, atoms on the surface often have the remaining bonding capacity. Thus, the adsorption of gas on the

Received: April 18, 2022

Accepted: May 30, 2022

Published: June 9, 2022



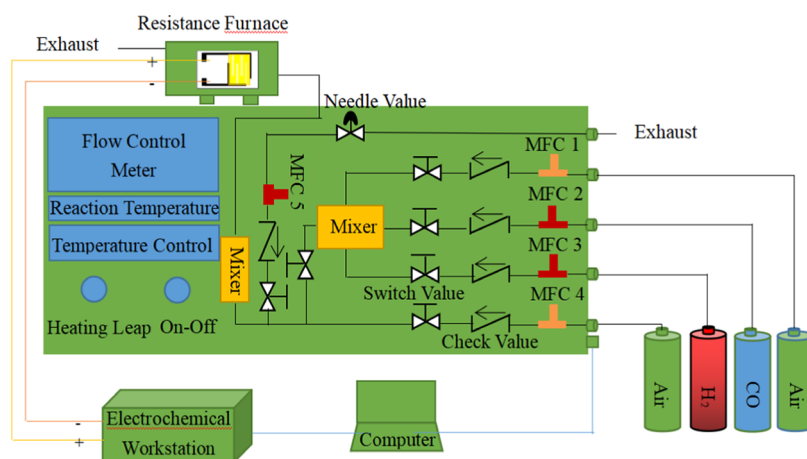


Figure 1. Schematic diagram of the measurement apparatus for the gas adsorption sensing response.

semiconductor can cause some physical properties to change. For example, adsorption of gas on the semiconductor can cause the surface conductivity to change, which makes MOSs widely applicable as gas sensors.^{17–19} However, thus far, there is no report characterizing the adsorption behavior by employing the GSR.

In this paper, GSRs caused by the adsorption process are employed as a new method to capture some adsorption behaviors, which are impossible for the traditional methods to obtain. Based on the new method, three adsorption data mentioned above cannot be captured using traditional chemisorption instruments or other methods. Above all, the device in this work measures the change of the GSR during the adsorption process to capture adsorption information, which is reported for the first time.

2. EXPERIMENTAL SECTION

First, 5 g of tin tetrachloride pentahydrate ($\text{SnCl}_4 \cdot 5\text{H}_2\text{O}$) was dissolved in 100 mL of deionizing water, 0.5 g of citric acid ($\text{C}_6\text{H}_8\text{O}_7 \cdot \text{H}_2\text{O}$) was added as a dispersant, and 0.5 mol/L ammonia water was used as a precipitant to prepare the tin hydroxide precipitate. The precipitate was aged for 12 h, and the chloride ions were removed by washing several times. The precipitate was heated to 60 °C and dissolved in saturated oxalic acid ($\text{H}_2\text{C}_2\text{O}_4 \cdot 2\text{H}_2\text{O}$) until the precipitate was completely dissolved, and transparent SnO_2 sol was obtained. The transparent SnO_2 sol obtained by adding saturated polyethylene glycol as a surfactant was placed in a drying box and dried at 80 °C for 72 h to obtain the SnO_2 gel precursor. The obtained dry gel was incubated at 600 °C for 2 h to obtain SnO_2 nanopowder. The working conditions of the sensor are as follows: The sensing adsorption materials are tested in dry air at 400 °C. The gas concentration is presented in all figures. The test instrument and process can be seen in our previous work,³ as shown in Figure 1. The test system consists of two gas distribution devices, a test chamber, and an electrochemical workstation. The electrochemical workstation and the sensor element are connected with platinum wire electrodes, and the outlet of the secondary gas distribution device is connected with the test chamber. The system can achieve continuous and accurate gas distribution and testing of a wide range of target gases. The maximum flow rate of target gas such as H_2 and CO controlled by MFC2 and MFC3 is 20 mL/min. The maximum flow rate of background gas such as Air, N_2 and O_2 controlled by MFC1 and MFC4 is 1000 mL/

min. Thus, based on the test instrument, different concentration of target gas can be obtained accurately.

3. RESULTS AND DISCUSSION

Figure 2 represents the GSR after different gases are passed onto the surface of SnO_2 in different orders. First, 10 ppm H_2 is injected into the test furnace in which the SnO_2 materials are present. After the H_2 is adsorbed onto the SnO_2 surface and reaches adsorption equilibrium, 420 ppm CO is injected into the test furnace. After the two gases reach adsorption equilibrium, the SnO_2 current can be indexed as C_1 . Then, the two gases are removed at the same time, and the SnO_2 current returns to the ground state. Second, the ventilation sequence is reversed, that is, first, 420 ppm CO is injected into the test furnace, followed by 10 ppm H_2 ; after the two gases reach adsorption equilibrium, the SnO_2 current now can be indexed as C_2 . Interestingly, the two currents C_1 and C_2 under these two situations are the same. This indicates that the final state of CO and H_2 coadsorption is independent of the adsorption order. It also indicates that the adsorption of CO and H_2 is single-molecular layer adsorption, which can also be inferred further as follows. If the adsorption process belongs to multimolecular layer adsorption, CO and H_2 adsorbed on the SnO_2 surface will have different adsorption layer structures due to the different adsorption sequences, so the SnO_2 current C_1 and C_2 should be totally different. Therefore, the single-adsorption layer of gas adsorption can be inferred by GSR (here, SnO_2 current). To verify the conclusion, other two cases such as 100 ppm H_2 and 300 ppm CO and 50 ppm H_2 and 150 ppm CO are passed onto the surface of SnO_2 in different orders, as presented in Figure 1b,c. The same conclusion as in Figure 1a is obtained. This adsorption information cannot be captured using traditional chemisorption instrument.

Figure 3 represents the GSR caused by H_2 and CO after they are passed onto the surface of SnO_2 in different orders. First, 10 ppm H_2 is injected into the test furnace in which the SnO_2 materials are present. After the H_2 is adsorbed on the SnO_2 surface and reaches adsorption equilibrium, the SnO_2 current can be indexed as D_1 . Then, another 30 ppm H_2 is injected into the test furnace. After the above-mentioned 40 ppm H_2 gases reach adsorption equilibrium, the SnO_2 current can be indexed as D_2 . Then, the 40 ppm H_2 is removed, and the SnO_2 current returns to the ground state. Second, 440 ppm CO is injected into the test furnace to make the current same as the current caused by 10 ppm H_2 , indexed as D_3 , and then, 30 ppm

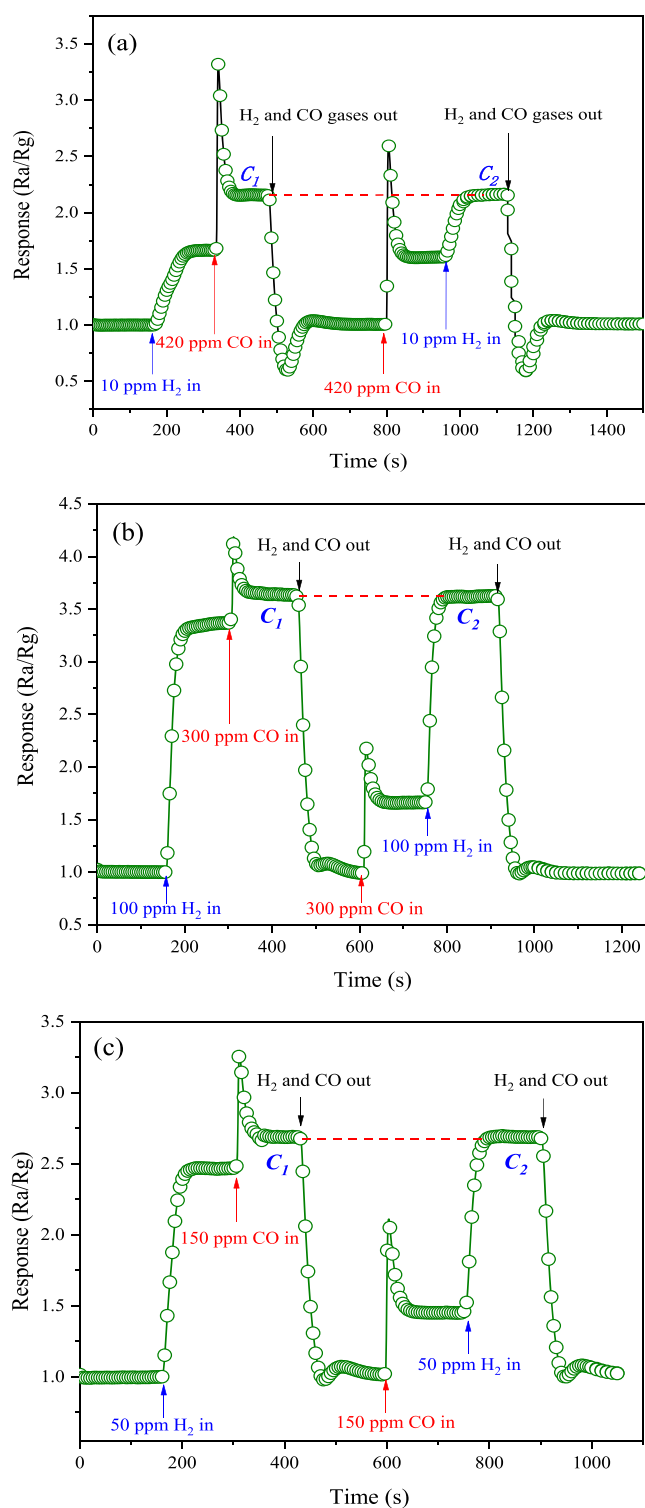


Figure 2. Gas sensing response caused by (a) 10 ppm H₂ and 420 ppm CO, (b) 100 ppm H₂ and 300 ppm CO, and (c) 50 ppm H₂ and 150 ppm CO adsorption after they are passed onto the surface of SnO₂ in different orders in the air background.

H₂ is injected into the test furnace; after the mixture of 440 ppm CO and 30 ppm H₂ reaches adsorption equilibrium, the SnO₂ current now can be indexed as D_4 . Interestingly, the response change caused by 30 ppm H₂ under the condition that the same current caused by 10 ppm H₂ or 440 ppm CO previously is not the same can be indexed as ΔA and ΔB ,

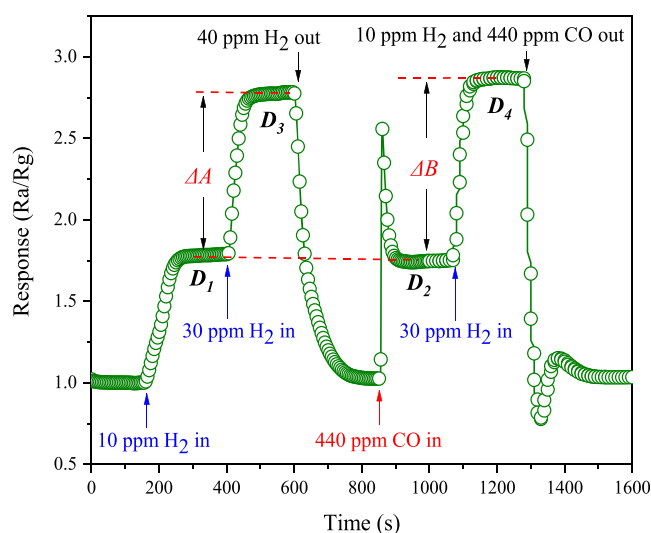


Figure 3. Gas sensing response caused by H₂ and CO adsorption after they are passed onto the surface of SnO₂ in different orders in the air background.

respectively, as shown in Figure 3. There is a slight difference between ΔA and ΔB , which may indicate that there are small interactions between CO and H₂. Therefore, the interaction between multicomponent gases during coadsorption can be inferred from the gas sensing behavior. This adsorption information cannot be captured using traditional chemisorption instruments or other methods.

Figure 4a represents the GSR caused by the adsorption of 100, 200, 300, 400, and 500 ppm H₂ on the SnO₂ sample surface under different carrier gas conditions. The curve in Figure 4a is fitted with the empirical formula $R = 1 + KC^n$ to obtain the quantitative relationship equation between the response value and the gas concentration, as shown in Figure 4b, where R represents the response of SnO₂, that is, the air-divided resistance in H₂, C is the gas concentration, and n is the exponent of the gas concentration. Taking the logarithm of both sides of $R = 1 + KC^n$, the n values are obtained. It can be found that the n value has a small relationship with the oxygen concentration in different carrier gases, which may indicate that the adsorption site of O₂ is totally different from that of H₂. Thus, the adsorption site and the adsorption behavior between two homogeneous gases can be obtained by evaluating the n value.^{1,21,22}

Figure 5 shows the adsorption sensing response kinetic curve of H₂ on the SnO₂ surface obtained by the GSR. The adsorption sensing response kinetic curve is obtained from Figure 4a as follows: taking the derivative of resistance with respect to time (dR/dt) versus time. From the figure, we can obtain the adsorption sensing response kinetic behavior of the H₂ gas in different oxygen concentrations. From the curves, we can see that with the increase of oxygen concentrations, the adsorption sensing response kinetics of H₂ decreases obviously. This is a new method to analyze the adsorption sensing response kinetic behavior in different gas concentrations. Above all, all the methods reported in this work may be promising to be employed in the explanation of catalysis, gas–solid reactions, and gas sensing mechanisms.

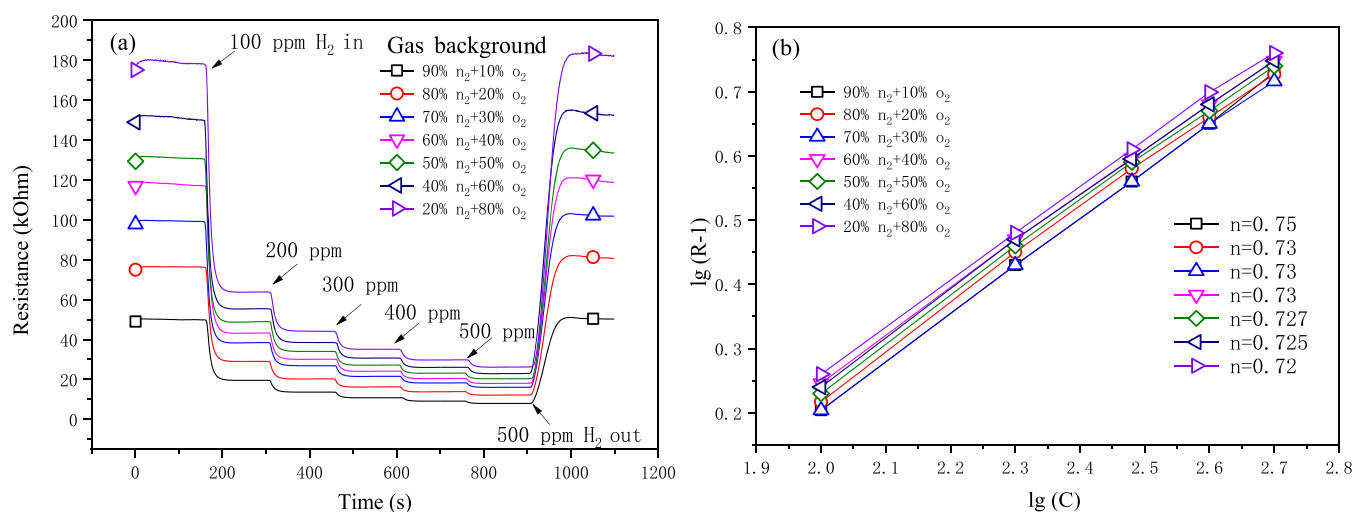


Figure 4. (a) Gas sensing electronic signal caused by H_2 adsorption in different oxygen concentrations. (b) n values obtained by taking the logarithm of both sides of $R = 1 + KC^n$.

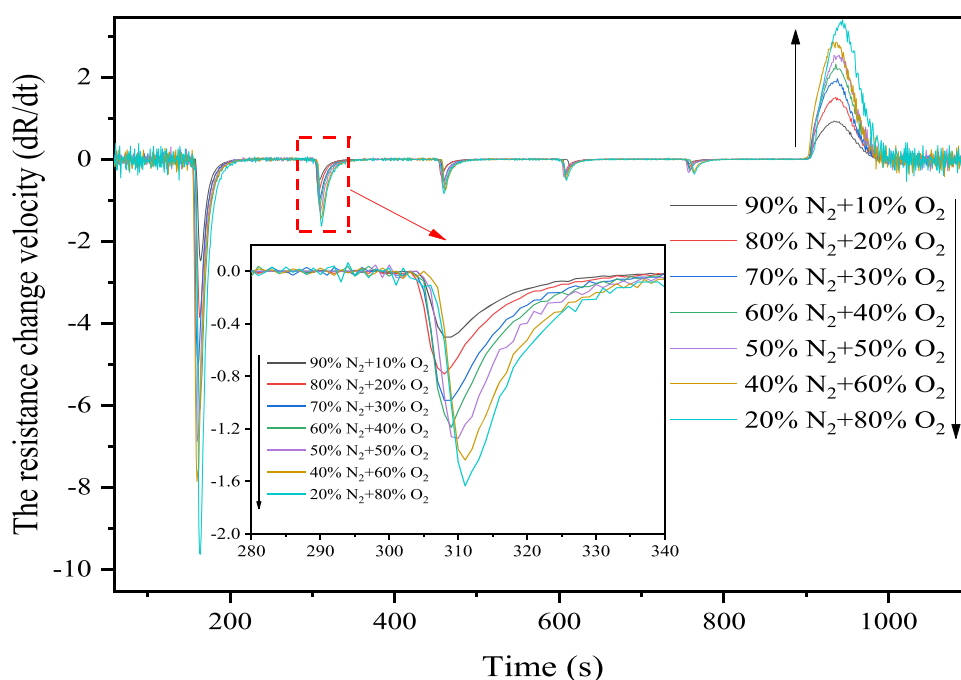


Figure 5. Adsorption sensing response velocity curve of H_2 on the SnO_2 surface obtained by the GSR.

4. CONCLUSIONS

In this paper, GSRs caused by the adsorption process are employed as a new method to capture some adsorption behaviors, which are impossible for the traditional methods to obtain. The following adsorption behaviors characterized by this new method are presented for the first time: (1) distinguishing the adsorption type using the examples of H_2 and CO: the single-adsorption layer of gas adsorption can be inferred by the GSR; (2) detecting the interaction between different gases: the interaction between multicomponent gases during coadsorption can be inferred from the gas sensing behavior; and (3) measuring the adsorption sensing response velocity based on the GSR. These three adsorption data mentioned above cannot be captured using traditional chemisorption instruments or other methods. Above all, the device in this work measures the change of the GSR during the

adsorption process to capture adsorption information, which is reported for the first time. These methods will be promising to provide original characterization data in the research fields such as heterogeneous catalysis, gas–solid reactions, and gas sensing mechanisms.

AUTHOR INFORMATION

Corresponding Authors

Xi-Tao Yin – School of Physics and Optoelectronic Engineering, Ludong University, Yantai, Shandong Province 264000, China; orcid.org/0000-0003-0991-8128; Email: yxtaj@163.com

Jing Li – The Key Laboratory of Chemical Metallurgy Engineering of Liaoning Province, University of Science and Technology Liaoning, Anshan, Liaoning Province 114051, China; Email: lijing_as321@163.com

Xiaoguang Ma – School of Physics and Optoelectronic Engineering, Ludong University, Yantai, Shandong Province 264000, China; orcid.org/0000-0002-7935-499X; Email: hsiaoguangma@ldu.edu.cn

Authors

Ying Liu – School of Physics and Optoelectronic Engineering, Ludong University, Yantai, Shandong Province 264000, China; orcid.org/0000-0003-3397-3207

Xiao-Ming Tan – School of Physics and Optoelectronic Engineering, Ludong University, Yantai, Shandong Province 264000, China

Xiao-Chun Gao – School of Physics and Optoelectronic Engineering, Ludong University, Yantai, Shandong Province 264000, China

Complete contact information is available at:

<https://pubs.acs.org/10.1021/acsomega.2c02405>

Notes

The authors declare no competing financial interest.

ACKNOWLEDGMENTS

Financial support is provided by the National Natural Science Foundation of China (Grant Nos. 51874169, 51974157, 52074153, 11674145), the Natural Science Foundation of Shandong Province (No. ZR2020KF025), and the Research Foundation for Advanced Talents of Ludong University (No. ZR2021019). We also thank the support of Shandong Youth Innovation Team Introduction and Education Program.

REFERENCES

- (1) Shimizu, Y.; Nakamura, Y.; Egashira, M. Effects of diffusivity of hydrogen and oxygen through pores of thick film SnO₂ based sensors on their sensing properties. *Sens. Actuators, B* **1993**, *13*, 128–131.
- (2) Yin, X.-T.; Li, J.; Dastan, D.; Zhou, W. D.; Garmestani, H.; Alamgir, F. M. Ultra-high selectivity of H₂ over CO with a p-n nanojunction based gas sensors and its mechanism. *Sens. Actuators, B* **2020**, *319*, No. 128330.
- (3) Yin, X.-T.; Li, J.; Wang, Q.; Dastan, D.; Shi, Z.-C.; Alharbi, N.; Garmestani, H.; Tan, X.-M.; Liu, Y.; Ma, X.-G. Opposite sensing response of heterojunction gas sensors based on SnO₂–Cr₂O₃ nanocomposites to H₂ against CO and its selectivity mechanism. *Langmuir* **2021**, *37*, 13548–13558.
- (4) Yamazoe, N.; et al. Effect of additives on semiconductor gas sensors. *Sens. Actuators* **1983**, *4*, 283–289.
- (5) Strässler, S.; Reis, A. Simple models for N-type metal oxide gas sensors. *Sens. Actuators* **1983**, *4*, 456–472.
- (6) Morrison, S. R. Selectivity in semiconductor gas sensors. *Sens. Actuators* **1987**, *12*, 425–440.
- (7) Kohl, D. Surface processes in the detection of reducing gases with SnO₂-based devices. *Sens. Actuators B* **1989**, *18*, 71–113.
- (8) Yamazoe, N. New approaches for improving semiconductor gas sensors. *Sens. Actuators B* **1991**, *5*, 7–19.
- (9) Shimizu, Y.; Kuwano, N.; Hyodo, T.; Egashira, M. High H₂ sensing performance of anodically oxidized TiO₂ film contacted with Pd. *Sens. Actuators, B* **2002**, *83*, 195–201.
- (10) Bârsan, N.; Hübner, M.; Weimar, U. Conduction mechanisms in SnO₂ based polycrystalline thick film gas sensors exposed to CO and H₂ in different oxygen backgrounds. *Sens. Actuators, B* **2011**, *157*, 510–517.
- (11) Rong, F.; Zhao, J.; Su, P.; Yao, Y.; Li, M.; Yang, Q.; Li, C. Zinc-cobalt oxides as efficient water oxidation catalysts: the promotion effect of ZnO. *J. Mater. Chem A* **2015**, *3*, 4010–4017.
- (12) Yang, C.; Wang, J.; Fan, H. L.; Shangguan, J.; Mi, J.; Huo, C. Contributions of tailored oxygen vacancies in ZnO/Al₂O₃ composites to the enhanced ability for H₂S removal at room temperature. *Fuel* **2018**, *215*, 695–703.
- (13) Haerifar, M.; Azizian, S. Mixed surface reaction and diffusion-controlled kinetic model for adsorption at the solid/solution interface. *J. Phys. Chem. C* **2013**, *117*, 8310–8317.
- (14) Yu, L.; Wang, L.; Xu, W.; Chen, L.; Fu, M.; Wu, J.; Ye, D. Adsorption of VOCs on reduced graphene oxide. *J. Environ. Sci.* **2018**, *67*, 171–178.
- (15) Zaera, F. The surface chemistry of metal-based hydrogenation catalysis. *ACS Catal.* **2017**, *7*, 4947–4967.
- (16) Arvaniti, I.; Netos, V.; Siokos, V.; Metaxa, E.; Kalantzopoulou, F. R. Relation between adsorption and catalysis in the case of NiO and Co₃O₄. *Appl. Surf. Sci.* **2010**, *256*, 5559–5565.
- (17) Muttakin, M.; Pal, A.; Rupa, M. J.; Ito, K.; Saha, B. B. A critical overview of adsorption kinetics for cooling and refrigeration systems. *Adv. Colloid Interface Sci.* **2021**, *294*, No. 102468.
- (18) Rupa, M. J.; Pal, A.; Mitra, S.; Saha, B. B. Time adapted linear driving force model for gas adsorption onto solids. *Chem. Eng. J.* **2021**, *420*, No. 129785.
- (19) Rupa, M. J.; Pal, A.; Saha, B. B. Activated carbon-graphene nanoplates based green cooling system: Adsorption kinetics, heat of adsorption, and thermodynamic performance. *Energy* **2020**, *193*, No. 116774.
- (20) Yin, X.-T.; Lv, P.; Li, J.; Jafari, A.; Wu, F.-Y.; Wang, Q.; Dastan, D.; Shi, Z.-C.; Yu, S.-T.; Garmestani, H. Nanostructured tungsten trioxide prepared at various growth temperatures for sensing applications. *J. Alloys Compd.* **2020**, *825*, No. 154105.
- (21) Shimizu, Y.; Maekawa, T.; Nakamura, Y.; Egashira, M. Effects of gas diffusivity and reactivity on sensing properties of thick film SnO₂-based sensors. *Sens. Actuators, B* **1998**, *46*, 163–168.
- (22) Yin, X.-T.; Zhou, W.-D.; Li, J.; Wang, Q.; Wu, F.-Y.; Dastan, D.; Wang, D.; Garmestani, H.; Wang, X.-M.; Talu, S. A highly sensitivity and selectivity Pt-SnO₂ nanoparticles for sensing applications at extremely low level hydrogen gas detection. *J. Alloys Compd.* **2019**, *805*, 229–236.